



**Magnetic design evolution in perpendicular magnetic recording media as revealed by resonant small angle x-ray scattering**

Tianhan Wang, Virat Mehta, Yoshihiro Ikeda, Hoa Do, Kentaro Takano, Sylvia Florez, Bruce D. Terris, Benny Wu, Catherine Graves, Michael Shu, Ramon Rick, Andreas Scherz, Joachim Stöhr, and Olav Hellwig

Citation: *Applied Physics Letters* **103**, 112403 (2013); doi: 10.1063/1.4820921

View online: <http://dx.doi.org/10.1063/1.4820921>

View Table of Contents: <http://scitation.aip.org/content/aip/journal/apl/103/11?ver=pdfcov>

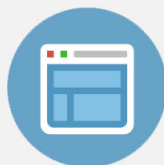
Published by the [AIP Publishing](#)

---



## Re-register for Table of Content Alerts

Create a profile.



Sign up today!



## Magnetic design evolution in perpendicular magnetic recording media as revealed by resonant small angle x-ray scattering

Tianhan Wang,<sup>1,2</sup> Virat Mehta,<sup>3</sup> Yoshihiro Ikeda,<sup>3</sup> Hoa Do,<sup>3</sup> Kentaro Takano,<sup>3</sup> Sylvia Florez,<sup>3</sup> Bruce D. Terris,<sup>3</sup> Benny Wu,<sup>2,4</sup> Catherine Graves,<sup>2,4</sup> Michael Shu,<sup>2,4</sup> Ramon Rick,<sup>2,4</sup> Andreas Scherz,<sup>2</sup> Joachim Stöhr,<sup>2,5</sup> and Olav Hellwig<sup>3</sup>

<sup>1</sup>Department of Materials Science and Engineering, Stanford University, Stanford, California 94035, USA

<sup>2</sup>Stanford Institute for Materials & Energy Science (SIMES), SLAC National Accelerator Laboratory, 2575 Sand Hill Road, Menlo Park, California 94025, USA

<sup>3</sup>San Jose Research Center, HGST a Western Digital company, 3403 Yerba Buena Rd., San Jose, California 95135, USA

<sup>4</sup>Department of Applied Physics, Stanford University, Stanford, California 94035, USA

<sup>5</sup>Linac Coherent Light Source, SLAC National Accelerator Laboratory, 2575 Sand Hill Road, Menlo Park, California 94025, USA

(Received 21 July 2013; accepted 27 August 2013; published online 10 September 2013)

We analyze the magnetic design for different generations of perpendicular magnetic recording (PMR) media using resonant soft x-ray small angle x-ray scattering. This technique allows us to simultaneously extract in a single experiment the key structural and magnetic parameters, i.e., lateral structural grain and magnetic cluster sizes as well as their distributions. We find that earlier PMR media generations relied on an initial reduction in the magnetic cluster size down to the grain level of the high anisotropy granular base layer, while very recent media designs introduce more exchange decoupling also within the softer laterally continuous cap layer. We highlight that this recent development allows optimizing magnetic cluster size and magnetic cluster size distribution within the composite media system for maximum achievable area density, while keeping the structural grain size roughly constant. © 2013 AIP Publishing LLC. [<http://dx.doi.org/10.1063/1.4820921>]

For longitudinal magnetic recording (LMR), grain size reduction has historically been the major pathway for increasing areal density in hard disk drive (HDD) media technology. In contrast, for current perpendicular magnetic recording (PMR) media, the grain size has remained more or less constant at 8–9 nm since its introduction in 2006.<sup>1</sup> PMR uses phase-segregated CoCrPt-based granular magnetic thin films with perpendicular anisotropy that consist of Co-rich magnetic grains and oxide based non-magnetic grain boundaries.<sup>2,3</sup> Owing to a more favorable demagnetization field geometry, PMR media allow for a tighter packing of the bits than LMR media. Further improvements resulted from the introduction of a soft (magnetic) underlayer (SUL) for higher write fields and a tighter out-of-plane easy-anisotropy-axis alignment among the CoCrPt grains down to an angular spread of below 3° in today's PMR media. Even though grain size scaling came to a hold after introducing PMR, areal density has been increased almost 5 fold from about 150 Gb/in<sup>2</sup> in 2006 to about 700 Gb/in<sup>2</sup> in 2012.

Additional density progress was driven by the introduction and optimization of a more complex and more functional magnetic layer structure; more specifically, by addition of a lower anisotropy more continuous reversal assist layer or magnetic cap layer (MCL) that is deposited on top of the higher anisotropy granular recording layer (GRL). This exchange-coupled-composite/continuous-granular-composite (ECC/CGC) media architecture<sup>4–10</sup> allows the use of even higher anisotropy materials for the GRL (ECC-effect)<sup>5,6</sup> combined with a more uniform inter-granular lateral exchange in the media via the MCL (CGC-effect).<sup>7,8</sup> In such ECC/CGC media architectures, the lateral magnetic correlations length (or also called magnetic cluster size) and

its distribution can now be optimized by separately tuning the magnetic properties and microstructure in the GRL and the MCL.<sup>4,9,10</sup>

Using resonant soft x-ray small angle x-ray scattering (SAXS) techniques, we show that with this advanced ECC/CGC media concept it is possible to fabricate laterally completely de-coupled grain structures within the GRL and then fine tune the degree of lateral exchange from grain to grain via the MCL optimization. We highlight that as the grains in the GRL become fully exchange decoupled, it is only possible to reduce the magnetic cluster size of the composite system further by reducing lateral exchange in the MCL as well.

Traditionally, in HDD development the lateral structural grain size and its distribution are obtained from plane-view transmission electron microscopy (TEM) analysis of a small area from the media,<sup>11</sup> while lateral magnetic correlation lengths (or magnetic cluster sizes) are separately extracted using minor hysteresis loop analysis based on a set of simplified assumptions about lateral dipolar interactions within the media layer.<sup>12</sup> Here, we employ a more direct single approach for extracting those media parameters by using resonant SAXS, which also provides information on the distribution of lateral magnetic correlation lengths otherwise only accessible indirectly via spin stand analysis of AC- or otherwise demagnetized media.<sup>13</sup>

SAXS is a powerful synchrotron based characterization technique that allows obtaining statistically averaged information about magnetic and structural correlation length within the various layers of the recording media.<sup>14–17</sup> To achieve this, we probe resonant magnetic as well as charge (non-magnetic) scattering with linearly polarized x-rays at the Co L3 absorption edge in a transmission geometry as

illustrated in Fig. 1(a). The linearly polarized x-rays can be expressed in the circular basis vectors as an equal superposition of left and right circularly polarized waves separated by a phase difference of  $\pi$ . The magnetic scattering contrast results from x-ray magnetic circular dichroism, while the charge contrast results from elemental absorption. The eventual polarization of the charge and magnetic scattered waves is orthogonal, and therefore they do not interfere to produce cross-terms.<sup>18,19</sup> The resulting diffraction pattern in the far-field reciprocal space is simply the linear combination of pure-magnetic and pure-charge scattering terms. By taking another diffraction pattern off resonance, we can normalize out the non-resonant charge scattering contributions to yield only the Co charge and magnetic correlation lengths. The SAXS measurements were also compared with TEM and minor hysteresis loop analysis.<sup>12</sup> While structural grain size and grain size distribution are in good quantitative agreement between TEM and SAXS, minor hysteresis loop analysis revealed a systematically larger magnetic cluster size<sup>20</sup> than SAXS. Relative trends were very reproducible though. The quantitative disagreement in absolute cluster size values is expected as the minor loop technique extracts the magnetic cluster size by comparing two different magnetic configurations from minor/major hysteresis loop analysis based on a set of simplifying assumptions about demagnetization fields<sup>12</sup> (rather than measuring the cluster size in an AC-demagnetized state).

Fig. 1(a) shows the setup for the SAXS measurements taken at BL13.3 at the Stanford Synchrotron Radiation Lightsource (SSRL). The incident linearly polarized x-rays were tuned to the Co L3 edge at 778.8 eV (on resonance) and 758.8 eV (off resonance) and the probe size FWHM was  $220 \mu\text{m}$  by  $70 \mu\text{m}$ . The out-of-plane AC-demagnetized media samples<sup>21</sup> deposited on soft-x-ray transparent SiN membrane substrates have a random and equal distribution of magnetic clusters with anti-parallel, out-of-plane magnetization. The subsequent scattering patterns were collected on a  $2048 \times 2048$  in-vacuum CCD detector with pixel size of  $13.5 \mu\text{m}$ . A steel cross beamstop was used to block the directly transmitted beam. The accumulation time for each

image is approximately 10 min. Due to the limited size of the CCD and loss of data from the beamstop, images were taken at 3 camera distances and stitched together in order to extend the reciprocal space detection angle,  $q$ , from  $1.1 \text{ nm}^{-1}$  to  $0.012 \text{ nm}^{-1}$ , which corresponds to 5.67 nm to 530 nm in real space. Although the SAXS measurements are performed in frequency space, the close-packed, granular nature of the sample with thin boundaries and anisotropic shapes ensures that the average correlation length is well matched to the average grain size, the same can be expected for the magnetic structures produced by AC-demagnetization.<sup>14,15</sup> As shown in Fig. 1(b), the inner on-resonance ring originates from the Co magnetic scattering and indicates the magnetic correlation length. Since the magnetic structure is essentially binary, consisting of alternating “up” and “down” clusters, the magnetic correlation length corresponds to twice the average magnetic cluster size. The outer ring is dominated by the charge scattering intensity that indicates the charge correlation length corresponding to average structural grain sizes. This term has both the resonant Co charge scattering intensity and the total non-resonant charge scattering intensity from all existing elements that contribute to the grain structure (media layer and granular Ru underlayers). Due to the highly segregated nature of the PMR media samples with columnar grains extending through most of the Ru underlayers as well, the non-resonant charge scattering is relatively strong and visible even in the off-resonance image. Naturally, the inner magnetic ring is absent in the off-resonance image. The scattering intensity is angularly integrated against  $q$  to produce the most probable (peak) structural and magnetic correlation lengths. The respective distributions, defined as the ratio of the standard deviation over mean, are then found by fitting the profiles with log-normal distributions.

In Fig. 2, we display SAXS results of the “GRL only” (Fig. 2(a)) versus the full media structure, i.e., MCL + GRL (Fig. 2(b)) for four different generations of PMR media covering roughly the time frame from 2007 (Gen1 about  $150 \text{ Gb/in}^2$  density) through 2012 (Gen4 about  $700 \text{ Gb/in}^2$  density). The corresponding extracted structural grain and

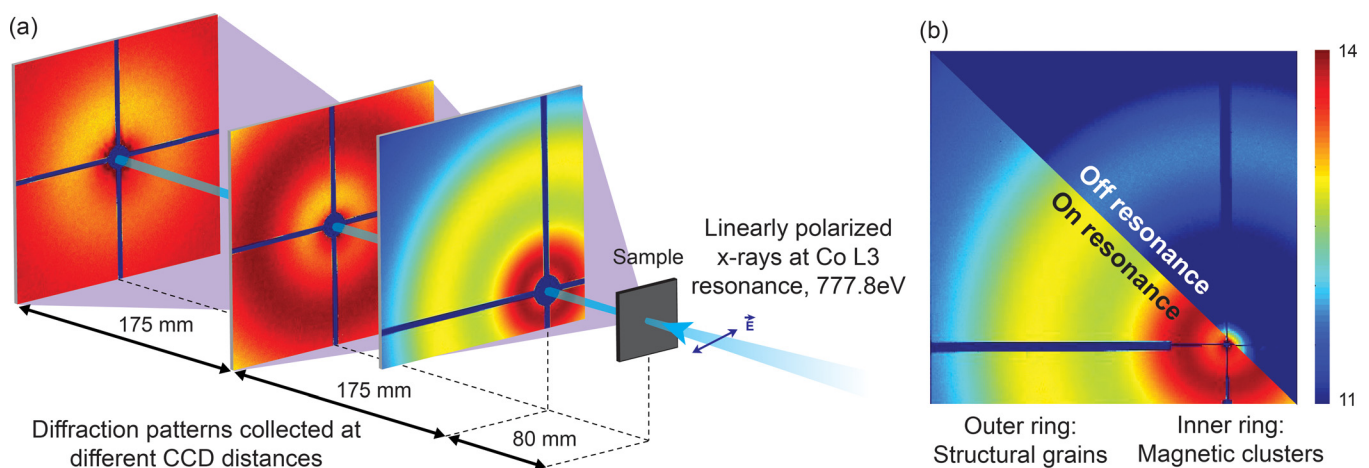


FIG. 1. (a) Experimental setup with CCD distances at 80, 255, and 430 mm from the sample. At the nearest distance, the CCD is off set to the upper left from the incoming beam in order to access the higher angles. (b) A comparison of resonant and non-resonant scattering showing the charge scattering ring corresponding to structural grains and the magnetic scattering ring corresponding to magnetic clusters. There is no magnetic scattering visible off resonance. The color bar represents the scattering intensity in logarithmic scale.

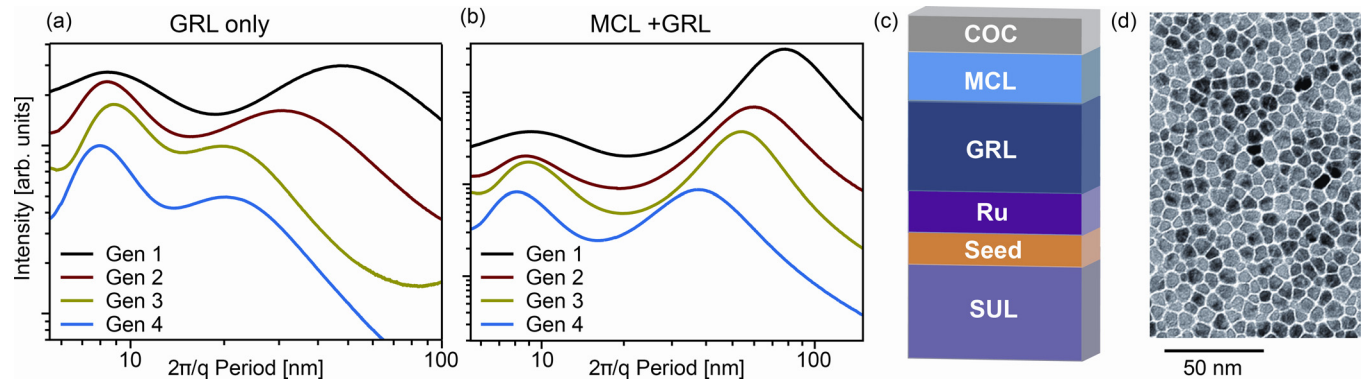


FIG. 2. (a) SAXS profiles for the GRL layer of 4 different generations of PMR recording media from 2007–2012 (Gen1–Gen4). (b) Corresponding profiles from the full media structures (GRL + MCL). SAXS features from the structural grains are visible at periods of around 8–10 nm, while SAXS features representing magnetic correlations, i.e., magnetic clusters are visible at periods of 20–100 nm. The intensities are shifted for better comparison. (c) A simplified magnetic media layer structure with SUL, seed and Ru underlayers, GRL, MCL, and carbon overcoat (COC). (d) Plan-view TEM image of the grain structure in the GRL from a recent Gen4 media design.

magnetic cluster parameters are listed in Table I and plotted versus media generation in Fig. 3.

For the SAXS data in Fig. 2, we observe that the grain size has remained more or less constant at 8–9 nm with the latest generation being closer to 8 nm. We obtain the grain size values for “GRL only” as well as for MCL + GRL media samples, since the more homogeneous MCL itself does not add any significant additional structural scattering at the grain size level. Furthermore, a continuous tightening of the grain size distribution over time (from Gen1 to Gen4) from initially 57% down to about 26% is evident from the data, which is consistent with plan-view TEM results from media layers obtained in the same time frame. An example for a plan-view TEM image of the GRL of a Gen4 type media is shown in Fig. 2(d).

For the magnetic cluster size of the full media structure (MCL + GRL), we observe a continuous shift to smaller values, from initially 38.8 nm down to 18.9 nm, as expected for recording media that supports increasingly higher areal density. While the SAXS of the “GRL only” shows a similar development to smaller magnetic cluster sizes for the first three media generations, the most recent Gen4 media does not reduce the magnetic cluster size in the GRL any further, thus revealing that most recently changes within the MCL have been driving the reduction in magnetic cluster size. Cluster sizes of the GRL basically have reached already the

minimum possible value (slightly larger than the grain size) for the Gen3 media, which represents complete magnetic decoupling of the structural grains in a Voronoi type of grain arrangement.<sup>22</sup> Further reduction of inter-granular exchange in the GRL is not possible and the only way to obtain an

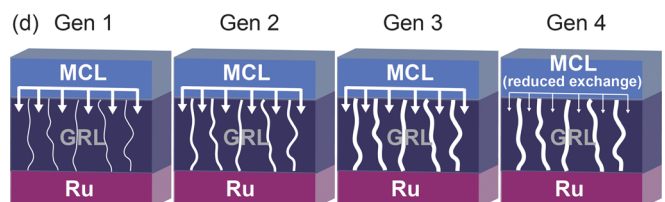
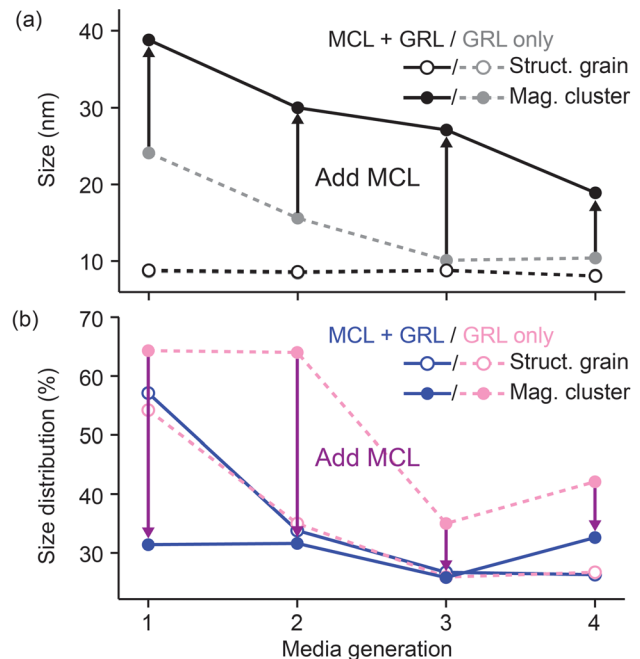


FIG. 3. (a) Average media grain sizes and cluster sizes as evolved over time from Gen1 to Gen4 for “GRL only” and full media stack (GRL + MCL). (b) Media grain size and cluster size distributions as evolved over time from Gen1 to Gen4 for “GRL only” and full media stack (GRL + MCL). (c) Illustration of simplified media layers and lateral microstructure as evolved over time from Gen1 to Gen4. From Gen1 through Gen3, the grain boundary phase in the GRL became more effective in magnetically decoupling the grains from each other. Moving to Gen4 media the only way to reduce lateral exchange further in the composite system is via the MCL.

TABLE I. Grain sizes/magnetic cluster sizes and grain size distributions/magnetic cluster size distributions as extracted from the SAXS data of Fig. 2.

Media generation/type		Gen1	Gen2	Gen3	Gen4
MCL + GRL	Grain size (nm)	8.8	8.6	8.8	8.1
	GS distribution (%)	57.1	33.8	26.7	26.3
	Cluster size (nm)	38.8	30.0	27.1	18.9
	CS distribution (%)	31.4	31.6	25.8	32.6
	Grains per cluster	19.4	12.2	9.5	5.4
GRL only	Grain size (nm)	8.7	8.5	8.8	8.1
	GS distribution (%)	54.2	35.0	25.9	26.7
	Cluster size (nm)	24.1	15.6	10.1	10.4
	CS distribution (%)	64.3	64.0	35.0	42.1
	Grains per cluster	7.7	3.4	1.3	1.6

additional reduction in magnetic cluster size for the composite media system (GRL + MCL) is by decreasing the lateral exchange within the MCL as illustrated in Fig. 3(c) for the Gen4 media structure.

However, a reduced lateral exchange in the MCL will in turn weaken the exchange averaging effect that is responsible for creating a tight distribution of cluster sizes. As a result, we observe an opposite trend towards a larger cluster size distribution in the most recent Gen4 media. However, overall this development has allowed an additional increase in areal density for the composite (GRL + MCL) media system. The effect of further reduced magnetic cluster size at the expense of a modestly increased cluster size distribution is illustrated in Fig. 3 by comparing the changes in magnetic cluster size and magnetic cluster size distribution when adding the MCL to the GRL.

In conclusion, we have shown that based on the simplified media structure considered here and the fact that the grain size has been more or less constant at a level of 8–9 nm since the introduction of PMR, additional media areal density gain originates from magnetic cluster size reduction, while keeping magnetic cluster size distribution at the same level of about 30%. However, for further future improvements in areal density it will be very important to decrease the magnetic cluster size by reducing the grain size in the GRL and maintaining tight distributions of grain size and magnetic cluster size. This has been proven very difficult within the current PMR paradigm, so that future technologies such as Heat Assisted Magnetic Recording (HAMR) or Bit Patterned Recording (BPR) may be necessary in order to push areal densities significantly beyond 1 Tb/in<sup>2</sup>.

SAXS continues to be a very powerful technique that provides simultaneous information about the charge and magnetic lateral microstructure in advanced PMR media systems. Comparing magnetic cluster size and cluster size distribution in the “GRL only” with the “GRL + MCL composite media system,” we could reveal the evolution in PMR media design from its introduction in 2006 until today.

The authors acknowledge support by the Department of Energy, Office of Basic Energy Sciences, under Contract No. DE-AC02-76SF00515. Portions of this research were carried out at the Stanford Synchrotron Radiation Lightsource, a Directorate of SLAC National Accelerator Laboratory and

an Office of Science User Facility operated for the U.S. Department of Energy Office of Science by Stanford University.

- <sup>1</sup>G. Bertero, R. Acharya, S. Malhotra, K. Srinivasan, E. Champion, G. Lauhoff, and M. Desai, “Double exchange-break PMR media structures,” in the 21st Magnetic Recording Conference (TMRC), 2010.
- <sup>2</sup>S. N. Piramanayagam, *J. Appl. Phys.* **102**, 011301 (2007).
- <sup>3</sup>A. Moser, K. Takano, D. T. Margulies, M. Albrecht, Y. Sonobe, Y. Ikeda, S. Sun, and E. E. Fullerton, *J. Phys. D: Appl. Phys.* **35**, R157 (2002).
- <sup>4</sup>T. P. Nolan, B. F. Valcu, and H. J. Richter, *IEEE Trans. Magn.* **47**, 63 (2011).
- <sup>5</sup>D. Suess, J. Lee, J. Fidler, and T. Schrefl, *J. Magn. Magn. Mater.* **321**, 545 (2009).
- <sup>6</sup>T. Hauet, S. Florez, D. Margulies, Y. Ikeda, B. Lengsfeld, N. Supper, K. Takano, O. Hellwig, and B. D. Terris, *Appl. Phys. Lett.* **95**, 222507 (2009).
- <sup>7</sup>Thomas P. Nolan, Bogdan F. Valcu, and Hans J. Richter, *IEEE Trans. Magn.* **47**, 63 (2011).
- <sup>8</sup>R. H. Victora and X. Shen, *IEEE Trans. Magn.* **41**, 2828 (2005).
- <sup>9</sup>G. Choe, J. Park, Y. Ikeda, B. Lengsfeld, T. Olson, K. Zhang, S. Florez, and A. Ghaderi, *IEEE Trans. Magn.* **47**, 55 (2011).
- <sup>10</sup>G. Choe, Y. Ikeda, K. Zhang, K. Tang, and M. Mirzamaani, *IEEE Trans. Magn.* **45**, 2694 (2009).
- <sup>11</sup>K. Tang, X. Bian, G. Choe, K. Takano, M. Mirzamaani, G. Wang, J. Zhang, Q.-F. Xiao, Y. Ikeda, J. Risner-Jamtegaard, and X. Xu, *IEEE Trans. Magn.* **45**, 786 (2009).
- <sup>12</sup>H. Nemoto, I. Takekuma, H. Nakagawa, T. Ichihara, R. Araki, and Y. Hosoe, *J. Magn. Magn. Mater.* **320**, 3144–3150 (2008).
- <sup>13</sup>M. Hashimoto, N. Ito, H. Kashiwase, T. Ichihara, H. Nakagawa, and K. Nakamoto, *IEEE Trans. Magn.* **46**, 1576 (2010).
- <sup>14</sup>O. Hellwig, J. B. Kortright, D. T. Margulies, B. Lengsfeld, and E. E. Fullerton, *Appl. Phys. Lett.* **80**, 1234 (2002).
- <sup>15</sup>E. E. Fullerton, O. Hellwig, Y. Ikeda, B. Lengsfeld, K. Takano, and J. B. Kortright, *IEEE Trans. Magn.* **38**, 1693 (2002).
- <sup>16</sup>E. E. Fullerton, O. Hellwig, K. Takano, and J. B. Kortright, *Nucl. Instrum. Methods Phys. Res. B* **200**, 202 (2003).
- <sup>17</sup>J. B. Kortright, O. Hellwig, D. T. Margulies, and E. E. Fullerton, *J. Magn. Magn. Mater.* **240**, 325 (2002).
- <sup>18</sup>J. B. Kortright, “Resonant soft X-ray and extreme ultraviolet magnetic scattering in nanostructured magnetic materials: Fundamentals and directions” *J. Electron Spectrosc. Relat. Phenom.* <http://dx.doi.org/10.1016/j.elspec.2013.01.019> (published online).
- <sup>19</sup>J. Stohr and H. C. Siegmann, *Magnetism From Fundamentals to Nanoscale Dynamics* (Springer, Berlin, 2006).
- <sup>20</sup>For “GRL only” data, we found with minor hysteresis loop analysis in average a cluster size that was by a factor of 1.48 larger than that extracted from SAXS, while for the full media structure (GRL + MCL) this factor was reduced to 1.26.
- <sup>21</sup>Demagnetization was performed by reducing the amplitude of an external magnetic field aligned normal to the sample surface from initially 15 kOe down to 10 Oe in 0.1% steps, while switching the field polarity back and forth between positive and negative at about 0.5 Hz.
- <sup>22</sup>M. F. Toney, K. A. Rubin, S.-M. Choi, and Ch. J. Glinka, *Appl. Phys. Lett.* **82**, 3050 (2003).